Alt, J.C., Kinoshita, H., Stokking, L.B., and Michael, P.J. (Eds.), 1996
Proceedings of the Ocean Drilling Program, Scientific Results, Vol. 148

2. GEOCHEMISTRY OF LAVAS FROM HOLE 896A[1]

T.S. Brewer,[2] W. Bach,[3] and H. Furnes[4]

ABSTRACT

Hole 896A is a second deep basement hole within oceanic crust formed at the Costa Rica Rift, which penetrated ~290 m of the lava sequence. The lava sequence is dominated by pillow lavas and massive flows, although minor breccias and two thin dikes were also recovered. The basalts are predominantly plagioclase + olivine phyric tholeiites, although in one section of the hole (353.1–392.1 mbsf) clinopyroxene is also present as phenocrysts.

Geochemically, the basalts are strongly depleted, moderately evolved mid-ocean ridge basalts. All the basalts are similar to the Groups D and D' basalts recovered from nearby Hole 504B, located approximately 1 km to the north of Hole 896A. None of the Hole 896A basalts have chemical signatures similar to the more evolved Group M or T basalts recovered from Hole 504B.

A significant geochemical feature of the Hole 896A basalts is that the drilled section can be divided into a number of discrete chemical units. The uppermost unit, Group A (<340 mbsf) has a relatively uniform composition, although the more primitive lavas occur at the top of this unit. Below 340 mbsf, the chemostratigraphy is characterized by sawtoothed profiles, produced by fractionation (plagioclase + olivine + clinopyroxene) followed by replenishment of the magma chamber. Near to the base of the current drilled section, the lowermost unit (Unit E) is geochemically similar to Unit B, except that the more primitive lavas occur at the top of this unit. Unit E is separated from the remainder of the drilled section by a thin highly depleted unit (Unit D).

The new geochemical data suggest that magmatism at the Costa Rica Rift developed in a dynamic system, where melts were produced from a common source by similar degrees of melting, but higher level processes (i.e., fractional crystallization and or mixing) generated discrete magma batches. This variation in the chemistry of the individual magma batches probably reflects a difference in the crustal level of the individual magma chambers and/or the timing of replenishment of the magma chambers.

INTRODUCTION

In the equatorial east Pacific, the Cocos-Nazca Spreading Center consists of the Galapagos, Ecuador and Costa Rica Rifts (Dick, Erzinger, Stokking, et al., 1992). This rift system was initiated approximately 27 Ma ago, by the formation of the Galapagos Triple Junction (Hey et al., 1977; Lonsdale and Klitgord, 1978), which produced a triangular wedge, the Galapagos Gore (Holden and Dietz, 1972; Dick, Erzinger, Stokking, et al., 1992). The Costa Rica Rift is the easternmost of the three rift segments, and separates the Cocos and Nazca plates. This rift system spreads asymmetrically at an intermediate rate (half rate of 3.6 cm/yr to the south and 3.0 cm/yr to the north).

With the drilling of Ocean Drilling Program Hole 896A, two deep basement holes (i.e., Holes 504B and 896A) now penetrate oceanic crust formed at the Costa Rica Rift. Hole 504B, the deepest basement hole in oceanic crust so far drilled, is located approximately 200 km to the south of the Costa Rica Rift, in 5.9 Ma old crust. Hole 896A is located approximately 1 km to the south of Hole 504B in crust ~2.8 $\times 10^4$ yr older than at Hole 504B. The distribution of the two holes provides an excellent opportunity to evaluate the nature of the magmatic processes operating at the Costa Rica Rift system and to evaluate if and how these processes varied in a relatively short period of time (i.e., <30,000 yr).

Hole 896A is located ~1 km southeast of Hole 504B on a bathymetric high overlying a basement topographic high (Alt, Kinoshita, Stokking, et al., 1993). Basement was first reached at 179 m below seafloor (mbsf), but the hole was cored from only 195.1 to 469 mbsf (Alt, Kinoshita, Stokking, et al., 1993). The actual depth of the basement may be more accurately constrained following detailed analysis of the geochemical wireline logs (T.S. Brewer and P.K. Harvey, pers. comm., 1993). Within the drilled section, core recovery averaged 26.9%. Pillow lavas (57%) and massive flows (38%) dominant the cored material, with breccias (5%) and two small dikes accounting for the remainder of the material. The basalts are sparsely to highly phyric tholeiites, with plagioclase and olivine dominating the phenocryst assemblages, although between 353.1 and 392.1 mbsf, clinopyroxene is present as a phenocryst phase (Alt, Kinoshita, Stokking, et al., 1993). With the exception of the glassy pillowed rims, the majority of the rocks are slightly altered (<10%) and variably veined (Alt, Kinoshita, Stokking, et al., 1993).

GEOCHEMISTRY

In all 109 samples which span the entire cored interval (Table 1) were analyzed from Hole 896A. All samples were crushed and then ground in agate; pressed powder pellets were used for the trace element analysis, major elements were determined on glass fusion beads, and major and trace elements were determined by X-ray fluorescence spectrometry at Nottingham University (Table 1) following identical procedures to those described in Alt, Kinoshita, Stokking, et al. (1993). The exceptions to this were in the determination of Nb and Rb, because in the data of Alt, Kinoshita, Stokking, et al. (1993) many of the samples were close to or below the level of detection for both of these elements. In an attempt to improve the quality of the Nb and Rb data, the count times were increased by a factor of 10 and each sample was analyzed 6 times. This procedure lowered the detection

[1]Alt, J.C., Kinoshita, H., Stokking, L.B., and Michael, P.J. (Eds.), 1996. *Proc. ODP, Sci. Results,* 148: College Station, TX (Ocean Drilling Program).

[2]Borehole Research, Department of Geology, University of Leicester, Leicester, LE1 7RH, United Kingdom. tsb5@leicester.ac.uk

[3]GeoForschungsZentrum Potsdam, Projektbereich 4.2, Telegrafenberg A50, D-14473 Potsdam, Federal Republic of Germany (present address: Universität Potsdam, Institut für Geowissenschaften, Postfach 601553, D-14415 Potsdam, Federal Republic of Germany). wbach@gfz-potsdam.de

[4]Geological Institute, University of Bergen, Allegaten 41, N-5007 Bergen, Norway. Harald.Furnes@geol.uib.no

Table 1. Geochemical analysis of basalts from Hole 896A.

Core, section, interval (cm)	Piece no.	Depth (mbsf)	SiO_2	Al_2O_3	TiO_2	Fe_2O	MgO	CaO	Na_2O	K_2O	MnO	P_2O	LOI	Ba	Ce	Cr	Cu	Ga
148-896A-																		
1R-1, 7–14	3	195.17	50.1	18	0.7	8.1	7.9	12	2.1	0.3	0.1	0	0.63	0	16	385	93	13
1R-1, 14–21	4	195.24	49.3	17	0.7	8.5	7.8	13	2	0.1	0.1	0.1	0.81	0	12	379	91	15
1R-1, 29–36	7	195.39	49.4	18	0.7	8.3	7.2	13	2.1	0.1	0.2	0.1	1.06	0	20	395	81	15
1R-1, 47–55	11	195.57	49.4	17	0.7	8.7	7.2	13	2	0.1	0.1	0	0.95	0	0	399	99	14
1R-1, 77–80	17	195.87	49.3	17	0.7	8.7	7	14	1.9	0.1	0.2	0	1.08	13	0	529	87	13
2R-1, 30–32	7	201.2	49.4	18	0.7	8.6	7.2	14	2	0.1	0.2	0.1	0.93	13	39	379	87	14
2R-1, 41–50	10	201.31	49.8	17	0.7	8.3	7.2	13	2	0.1	0.1	0	0.75	12	15	407	100	12
2R-1, 94–101	21	201.84	49	17	0.7	8.8	8.2	13	1.9	0.1	0.2	0	1	0	0	376	96	14
3R-1, 38–41	7	210.28	49.2	17	0.7	9.1	8.7	13	1.8	0	0.2	0	0.76	0	8	369	99	13
4R-1, 68–70	9C	219.58	49	17	0.7	8.9	7.6	13	1.9	0.1	0.2	0	0.98	9	0	384	89	14
5R-2, 38–40	1D	229.7	49.7	17	0.7	9	7.9	13	1.8	0	0.2	0	0.55	16	0	371	97	14
5R-2, 74–77	2	230.06	49.3	17	0.7	9	7.5	13	1.9	0.1	0.2	0	0.78	15	0	365	88	15
6R-1, 52–54	5C	238.42	49.4	17	0.7	9.2	7.7	13	1.8	0.1	0.2	0	0.99	0	18	387	98	14
6R-2, 89–91	10A	240.27	49.3	17	0.7	9.1	7.3	14	1.9	0.1	0.2	0	0.76	14	12	385	99	15
7R-1, 58–60	10A	247.98	49	17	0.7	9.2	7.2	14	1.9	0	0.2	0	1	23	9	387	92	14
7R-1, 80–83	13	248.2	49.3	17	0.7	9.2	7.8	13	1.8	0.1	0.2	0	0.93	35	21	363	93	14
8R-1, 29–32	7	257.39	49.1	17	0.8	8.7	7.2	14	1.9	0.1	0.2	0	0.83	8	21	406	95	13
9R-1, 138–141	25	268.08	49	16	0.7	9.5	8.4	13	1.9	0.1	0.2	0	1.13	16	8	379	95	13
9R-2, 29–33	3	268.43	48.1	16	0.7	9.4	9.2	12	1.7	0.1	0.2	0.1	2.58	0	0	366	72	11
10R-1, 116–118	9C	277.56	48.7	16	0.7	9.5	7.9	13	1.8	0.1	0.2	0	1.11	0	14	366	98	14
11R-1, 98–109	8B	286.98	49.2	17	0.7	9.4	7.2	13	1.9	0.1	0.2	0.1	1.03	11	29	361	80	15
11R-3, 12–17	3	289.04	49.5	16	0.8	9.4	7.5	13	1.9	0.1	0.2	0	1.15	20	0	387	100	16
11R-3, 30–35	5	289.22	49	16	0.8	9.9	8.1	13	1.9	0.1	0.2	0.1	0.93	10	17	343	78	17
11R-3, 48–53	8	289.4	48.6	16	0.7	9.4	8.6	13	1.8	0.1	0.2	0	1.23	16	0	367	90	16
12R-1, 78–81	10B	296.38	49	16	0.7	9.6	8.2	13	1.8	0.1	0.2	0	0.9	10	22	347	90	16
12R-2, 9–12	1C	297.14	49.8	16	0.7	9.2	8	13	1.9	0	0.2	0	0.61	0	22	353	95	15
14R-2, 38–41	2B	314.98	49.1	17	0.8	9.3	7.6	13	2	0.1	0.2	0.1	0.8	8	0	341	91	14
14R-2, 28–31	3	316.29	48.5	17	0.8	9.5	6.9	13	1.9	0.1	0.2	0	1.56	9	0	354	95	14
14R-2, 58–61	7	316.59	49.1	16	0.9	9.6	7.3	13	2	0.1	0.2	0.1	0.88	14	17	360	98	16
14R-2, 89–91	11B	316.6	48.7	18	0.8	9	7	13	2	0.1	0.2	0.1	0.86	13	0	364	76	15
14R-2, 113–115	16A	317.14	48.8	17	0.7	9.7	7.8	13	1.9	0.1	0.2	0	0.83	12	0	342	96	14
14R-3, 21–24	4	317.69	48.7	17	0.7	9.5	7.7	13	1.9	0.1	0.2	0.1	1.19	13	24	332	62	15
15R-1, 23–29	4	324.53	49	17	0.8	9.1	6.9	14	2	0.1	0.2	0	0.78	13	13	346	97	14
15R-1, 94–97	14	325.24	49	17	0.8	9.4	7.2	13	1.9	0.1	0.2	0.1	0.91	12	39	328	79	15
15R-1, 103–106	15	325.33	48.8	17	0.8	9.5	7.2	13	1.8	0	0.2	0	0.81	9	20	334	92	14
15R-1, 122–126	18	325.52	49.2	17	0.8	9	7.1	13	2	0.1	0.2	0.1	1.01	0	24	362	78	16
16R-1, 31–34	3B	334.21	49.9	16	0.8	9.3	8.1	13	1.8	0.1	0.2	0	0.4	14	0	335	67	13
16R-2, 61–64	1E	335.86	48.8	17	0.7	9.9	7.9	13	1.9	0	0.2	0.1	0.83	16	8	287	62	15
16R-3, 88–91	4B	337.58	49.2	16	0.7	9.5	8	13	1.8	0	0.2	0	0.68	17	15	328	76	14
17R-1, 1–3	1A	343.51	49.6	16	0.9	9.4	8	13	2.1	0.1	0.2	0.1	0.48	19	0	307	82	15
17R-1, 82–84	10B	344.32	50.3	15	0.9	9.4	8.7	13	1.9	0.1	0.2	0.1	0.08	18	0	317	113	15
17R-3, 89–93	8	347.33	49.9	16	0.9	9.5	8.2	13	1.9	0.1	0.2	0.1	0.1	25	0	293	87	13
17R-4, 53–58	3B	348.43	50	16	0.9	10	7.9	13	1.8	0.2	0.2	0.1	0.28	25	12	283	61	15
17R-4, 99–102	9	348.89	49.4	15	0.9	10	7.6	13	2.1	0.2	0.2	0.1	0.55	26	8	301	63	16
17R-4, 113–116	11	349.03	49.6	16	0.9	9.8	7.4	13	2.1	0.2	0.2	0.1	0.58	29	19	282	48	17
18R-1, 72–75	6B	353.82	49.8	16	1	9.9	8.4	13	1.9	0.1	0.2	0.1	0.3	28	0	318	74	17
18R-1, 142–145	12B	354.52	49.4	16	0.9	10	8.6	12	1.9	0.1	0.2	0.1	0.7	27	27	328	49	16
18R-2, 27–30	5	354.82	49.2	17	0.9	9.1	8.1	12	2.2	0.1	0.2	0.1	0.88	17	7	405	61	15
18R-2, 36–38	7	355.15	50.4	15	0.9	9.9	8.6	13	1.9	0	0.2	0.1	–0.1	0	14	331	74	15
19R-1, 111–115	18	356.23	49.7	15	0.9	10	8.7	13	1.8	0	0.2	0.1	0.15	22	30	316	66	14
19R-1, 36–38	7	356.36	49.8	17	1	8.7	8	12	2.2	0.1	0.2	0.1	0.83	22	0	322	68	15
19R-1, 111–115	18	357.11	50.3	16	0.9	9.1	8.3	12	1.9	0.1	0.2	0.1	0.43	23	12	399	68	16
19R-2, 28–34	6	357.57	50.2	16	0.9	9.4	8.5	13	1.9	0.1	0.2	0.1	0.38	16	12	306	83	16
20R-1, 14–20	5	363.64	49.7	16	0.9	9.5	8.2	13	2	0.1	0.2	0.1	0.45	34	0	320	71	16
20R-1, 57–60	14	364.07	49.6	16	0.9	9.4	8.4	13	2	0.1	0.2	0.1	0.58	17	8	324	68	16
20R-1, 73–77	16	364.23	49.7	16	0.9	9.5	8	13	2	0.1	0.2	0.1	0.4	22	0	336	77	15
20R-1, 124–127	25	364.27	49.5	17	0.9	9.3	8	13	2	0.1	0.2	0.1	0.68	31	19	330	70	16
21R-1, 0–7	1	373	49.6	16	0.9	10	7.9	13	1.9	0.3	0.2	0.1	0.68	26	0	351	45	14
21R-1, 11–19	3	373.11	49.4	16	0.9	9.8	8.1	12	2	0.2	0.2	0.1	0.53	29	22	324	79	14
21R-1, 145–147	21	374.45	49.3	18	0.9	8	7.3	12	2.4	0.1	0.1	0.1	1.24	17	0	398	61	14
21R-2, 27–29	3B	374.75	49.5	18	0.9	8.6	6.9	13	2.4	0.1	0.2	0.1	0.9	13	24	395	89	15
21R-3, 11–14	2	376.09	49.1	16	0.9	9.7	7.9	13	2	0.1	0.2	0.1	0.7	12	0	368	69	13
21R-3, 22–24	4A	376.2	49.6	17	0.9	9.3	8.2	13	1.9	0.1	0.2	0.1	0.66	28	13	332	72	15
22R-1, 10–15	2	382.7	50.5	16	0.9	8.8	7.5	13	1.9	0	0.2	0.1	0.6	24	0	351	76	15
22R-1, 64–66	7A	383.24	49.6	16	0.9	9.8	8.5	13	1.9	0.1	0.2	0.1	0.63	18	24	371	72	13
22R-2, 13–17	2	384.22	50.5	16	0.9	8.6	8	13	1.9	0	0.2	0.1	0.58	12	11	287	71	15
22R-2, 81–88	12A	384.9	49.2	16	0.9	9.8	8.4	13	2	0.1	0.2	0.1	0.78	22	16	326	59	16
22R-2, 134–138	18A	385.43	49.8	16	0.9	9.6	7.9	13	2	0.1	0.2	0.1	0.43	9	20	343	83	16
22R-3, 87–90	9	386.46	48.8	16	0.9	10	7.9	13	2	0.1	0.2	0.1	0.76	21	0	385	60	16
22R-4, 31–35	4	387.33	49.3	16	0.9	10	8.5	12	2.1	0.1	0.1	0.1	0.8	22	0	324	134	13
22R-4, 43–49	6	387.45	48.8	17	0.9	9.4	7.8	12	2.4	0.1	0.2	0.1	1.23	13	24	327	68	16
23R-1, 81–85	11	392.91	48.8	17	0.8	9.8	7.2	13	2.3	0.1	0.2	0.1	1.08	22	8	387	95	14
23R-2, 136–138	16	394.93	48.5	17	0.9	9.3	7.6	12	2.3	0.1	0.2	0.1	1.38	14	23	355	61	14
23R-3, 7–13	1	395.07	48.1	16	0.8	9.4	7.6	13	2.3	0	0.2	0	1.66	13	0	349	70	14
23R-3, 63–66	9A	395.63	48.3	17	0.9	9.8	7.8	11	2.4	0.1	0.1	0.1	1.81	27	12	400	71	16
23R-3, 128–132	17	396.28	49.1	16	0.8	9.4	9.1	12	2	0	0.2	0	1.11	25	17	321	83	16
24R-1, 12–15	1	401.92	48.6	16	0.8	9.1	9.5	12	2	0	0.2	0.1	1.05	19	0	311	67	13
24R-1, 21–24	1	402.1	48.9	16	0.8	9.3	9.7	12	2	0	0.2	0	1.08	24	0	305	83	15
24R-1, 114–117	7	402.94	48.5	16	0.8	9.4	9.6	12	2	0	0.2	0.1	1.11	13	0	319	68	14
24R-2, 69–72	8	403.99	48.7	17	0.9	9.3	7.9	12	2.4	0.1	0.2	0.1	1.38	24	9	336	48	15
24R-3, 23–25	3	405.01	49.4	16	0.8	9.2	8.3	13	2.1	0	0.2	0	0.83	22	12	313	82	14
24R-4, 66–69	8	406.9	49.3	17	0.8	9.3	7.9	13	2.1	0	0.2	0.1	0.93	15	0	321	72	13
24R-5, 61–64	6	408.29	49.3	17	0.8	9.2	8.2	13	2.1	0	0.2	0	0.6	18	10	331	71	13
25R-1, 11–13	3	411.41	48.5	17	0.8	9.4	7.2	13	2.2	0.1	0.2	0.1	1.23	20	0	387	80	14
25R-1, 127–129	16	412.57	49.2	17	0.8	9.2	8.6	13	2.1	0	0.2	0.1	0.53	0	9	334	75	14
25R-2, 123–124	2	414.03	48.7	17	0.9	9.6	7.1	13	2.2	0	0.2	0	1.06	12	0	347	81	15
25R-3, 67–73	10	414.93	48.5	17	0.8	9.4	8.5	13	2	0.1	0.2	0	1.06	9	13	326	78	14
26R-1, 92–95	1	421.92	49.1	17	0.8	9.3	6.9	13	2.3	0.1	0.1	0	1.08	29	8	373	88	13

Table 1 (continued).

Core, section, interval (cm)	Piece no.	La	Nb	Ni	Pb	Rb	S	Sc	Sr	Th	U	V	Y	Zn	Zr
148-896A-															
1R-1, 7–14	3	0	0.76	181	5	2.38	812	48	70	0	0	230	18	56	40
1R-1, 14–21	4	0	0.47	125	7	2.99	454	48	69	5	0	239	23	53	43
1R-1, 29–36	7	0	0	189	0	0	1931	45	70	1	2	227	23	55	41
1R-1, 47–55	11	0	0.8	169	6	1.77	1007	49	66	0	0	232	21	63	37
1R-1, 77–80	17	0	0.12	162	0	2.18	1207	45	62	5	0	220	22	54	44
2R-1, 30–32	7	0	0	170	0	0	1672	41	68	1	0	215	22	55	41
2R-1, 41–50	10	0	0.63	174	7	2.18	952	47	72	3	2	237	22	62	44
2R-1, 94–101	21	7	0.75	179	4	3.16	806	40	67	3	0	217	20	57	38
3R-1, 38–41	7	0	0.66	182	9	2.08	922	40	61	3	0	213	21	59	41
4R-1, 68–70	9C	0	0.49	175	8	2.11	1060	44	66	2	2	226	20	60	41
5R-2, 38–40	1D	0	0.71	178	5	2.59	710	42	67	0	2	221	22	62	45
5R-2, 74–77	2	0	0.74	167	4	1.77	1042	45	63	1	0	232	21	60	38
6R-1, 52–54	5C	0	0.87	163	0	2.63	1135	41	63	4	0	214	24	53	48
6R-2, 89–91	10A	8	0.8	167	5	3.02	1077	37	63	0	2	231	22	62	45
7R-1, 58–60	10A	0	0.77	163	8	1.78	978	41	67	0	0	234	22	57	44
7R-1, 80–83	13	0	0.75	164	4	1.85	1006	46	72	4	0	234	21	61	43
8R-1, 29–32	7	0	0.86	164	8	2.53	1015	50	69	0	0	226	22	61	43
9R-1, 138–141	25	0	0.94	159	3	2.44	978	46	72	0	0	229	21	64	41
9R-2, 29–33	3	0	0.91	162	5	4.08	473	40	66	0	0	232	22	58	44
10R-1, 116–118	9C	0	0.61	154	0	2.87	2761	45	69	4	0	197	23	53	45
11R-1, 98–109	8B	0	0	155	0	0	1568	41	70	2	0	226	21	55	46
11R-3, 12–17	3	0	0.9	148	5	2.59	1080	46	70	2	2	260	24	68	45
11R-3, 30–35	5	0	0	136	0	0	166	36	61	0	2	235	24	49	42
11R-3, 48–53	8	0	0.6	161	5	2.95	804	44	61	2	2	224	20	61	42
12R-1, 78–81	10B	7	0.43	169	6	3.56	298	43	74	1	1	221	21	57	39
12R-2, 9–12	1C	6	0.69	166	4	1.79	1590	39	61	2	0	224	21	63	46
14R-2, 38–41	2B	0	0.92	156	7	2.39	797	42	64	0	0	238	23	59	47
14R-2, 28–31	3	0	0.73	152	6	2.13	835	46	67	2	0	246	22	67	44
14R-2, 58–61	7	0	0.99	109	4	2	1249	50	68	0	2	272	25	72	50
14R-2, 89–91	11B	0	0.59	148	0	2.38	1856	47	65	1	0	228	24	56	44
14R-2, 113–115	16A	0	0.52	151	7	3.17	140	39	65	1	0	225	24	61	40
14R-3, 21–24	4	0	0	148	0	0	309	40	65	0	0	221	23	52	39
15R-1, 23–29	4	4	0.04	162	7	2.54	868	44	68	1	0	231	22	62	44
15R-1, 94–97	14	0	0	147	0	0	1185	42	64	0	0	222	22	51	42
15R-1, 103–106	15	0	0.4	143	9	2.21	1038	48	64	0	0	238	23	60	45
15R-1, 122–126	18	0	0	149	0	0	1988	46	66	0	2	243	26	63	43
16R-1, 31–34	3B	0	0.75	164	7	2.62	147	38	62	1	2	253	25	65	49
16R-2, 61–64	1E	0	0.35	148	0	1.88	92	37	62	1	0	208	23	46	41
16R-3, 88–91	4B	4	0.51	161	4	1.66	94	38	76	1	0	232	22	56	40
17R-1, 1–3	1A	4	0.71	121	5	3.46	695	45	64	0	0	264	24	65	51
17R-1, 82–84	10B	0	0.4	183	10	3.06	921	43	58	0	0	284	26	75	52
17R-3, 89–93	8	0	0.61	132	6	3.53	571	44	61	0	0	260	24	70	53
17R-4, 53–58	3B	0	0	103	0	0	433	46	56	0	0	254	27	58	45
17R-4, 99–102	9	0	0.61	82	3	5.08	102	47	61	0	0	277	25	63	51
17R-4, 113–116	11	0	0	105	0	0	110	46	61	0	1	256	27	60	50
18R-1, 72–75	6B	6	0.71	120	4	3	1347	45	58	1	0	277	26	73	47
18R-1, 142–145	12B	0	0	100	0	0	1500	47	57	2	0	259	28	57	48
18R-2, 27–30	5	0	0.62	109	0	2.21	2214	47	63	3	0	272	28	64	52
18R-2, 36–38	7	0	0.71	129	7	1.66	1565	45	54	1	0	268	24	73	50
19R-1, 111–115	18	0	0.35	121	7	2.17	1195	43	53	2	0	266	26	66	47
19R-, 36–38	7	0	0.76	127	0	1.63	1792	47	61	5	0	262	29	68	53
19R-1, 111–115	18	0	0.78	120	0	2.48	1662	47	57	3	0	266	28	66	53
19R-2, 28–34	6	0	0.62	181	4	3.97	502	38	56	4	0	269	25	71	48
20R-1, 14–20	5	0	0.9	102	8	2.98	989	41	58	0	0	273	26	67	50
20R-1, 57–60	14	0	0.76	122	0	1.86	1632	44	58	4	0	258	27	67	56
20R-1, 73–77	16	5	0.54	93	5	2.41	1149	39	61	0	2	273	26	71	53
20R-1, 124–127	25	0	0.54	118	0	2.72	1781	45	58	3	0	246	27	68	47
21R-1, 0–7	1	0	0.74	98	0	7.46	126	42	55	0	0	248	27	65	52
21R-1, 11–19	3	0	0.86	109	8	5.23	581	46	61	0	0	267	25	67	52
21R-1, 145–147	21	0	0.52	98	0	3.43	2161	48	81	4	0	212	28	46	52
21R-2, 27–29	3B	0	0.68	138	7	3.41	550	39	81	1	0	220	22	66	49
21R-3, 11–14	2	0	0.35	113	0	3.12	1244	41	56	2	0	252	27	60	53
21R-3, 22–24	4A	0	0.83	118	7	2.43	1252	39	58	4	0	252	23	68	48
22R-1, 10–15	2	0	0.78	124	0	1.46	1008	42	53	2	2	253	26	56	50
22R-1, 64–66	7A	0	0.79	120	7	2.49	993	46	56	3	2	259	24	70	43
22R-2, 13–17	2	0	0.65	115	0	2	473	45	54	6	0	245	25	63	49
22R-2, 81–88	12A	7	0.52	102	5	4.06	121	38	59	0	0	262	26	63	48
22R-2, 134–138	18A	0	0.99	122	2	3.49	650	42	59	2	0	256	25	71	52
22R-3, 87–90	9	0	0.78	105	0	3.91	124	40	58	7	0	252	26	62	51
22R-4, 31–35	4	0	0.47	106	7	3.52	425	41	63	2	2	266	27	71	50
22R-4, 43–49	6	9	0.34	110	9	3.87	125	43	80	0	0	232	23	68	48
23R-1, 81–85	11	0	0.47	126	8	3.83	183	39	78	0	0	214	21	65	46
23R-2, 136–138	16	0	0.45	127	0	5.19	147	37	74	6	0	212	26	47	50
23R-3, 7–13	1	0	0.55	149	2	4.87	146	39	76	2	0	204	22	59	41
23R-3, 63–66	9A	0	0.86	93	0	9.71	205	43	74	5	0	222	28	51	47
23R-3, 128–132	17	0	0.73	157	9	1.52	1904	27	67	0	0	199	22	67	46
24R-1, 12–15	1	0	0.67	150	0	1.29	1408	40	62	2	0	182	24	39	49
24R-1, 21–24	1	0	0.63	157	6	1.53	1911	35	64	2	0	193	22	50	47
24R-1, 114–117	7	0	0.41	147	0	1.93	1682	36	62	5	0	185	22	40	48
24R-2, 69–72	8	0	0.45	129	0	7.28	108	40	72	4	0	226	26	50	49
24R-3, 23–25	3	0	0.78	162	4	2.07	1243	35	82	0	0	199	22	56	49
24R-4, 66–69	8	0	0.83	166	0	1.44	384	34	70	3	0	195	24	48	47
24R-5, 61–64	6	0	0.84	157	0	1.39	1364	32	67	3	0	186	24	46	49
25R-1, 11–13	3	0	0.58	187	0	2.76	1333	41	69	2	0	193	25	57	48
25R-1, 127–129	16	0	0.56	178	0	2.05	1710	39	70	2	0	190	22	48	46
25R-2, 123–124	2	0	0.73	192	4	2.19	938	43	72	1	0	196	20	59	48
25R-3, 67–73	10	0	0.74	181	0	2.76	1770	42	66	4	0	194	22	53	47
26R-1, 92–95	1	0	0.69	198	9	2.95	792	41	69	3	0	201	21	60	48

Table 1 (continued).

Core, section, interval (cm)	Piece no.	Depth (mbsf)	SiO_2	Al_2O_3	TiO_2	Fe_2O	MgO	CaO	Na_2O	K_2O	MnO	P_2O	LOI	Ba	Ce	Cr	Cu	Ga
26R-1, 134–139	1	422.34	49.2	17	0.9	9.5	6.7	13	2.3	0.1	0.2	0	0.88	32	0	394	93	14
26R-2, 88–89	2	423.39	48.4	17	0.9	9.6	7	13	2.2	0	0.2	0	1.34	38	7	367	81	14
27R-1, 22–25	1	430.72	48.9	17	0.9	9.9	7.2	13	2.2	0.1	0.2	0	1	14	0	364	89	15
27R-1, 71–75	1	431.21	49.8	16	0.8	9.8	8.4	13	1.9	0.3	0.2	0	0.4	29	15	378	74	14
27R-1, 86–92	10	431.36	48.7	16	0.6	9.1	9	13	1.8	0.4	0.2	0.1	1.26	13	0	367	64	11
27R-1, 101–104	12B	431.51	49.2	16	0.8	9.3	8.3	13	1.9	0.2	0.2	0.1	0.78	12	0	365	68	13
27R-2, 109–112	2	433.04	48.9	16	0.6	9.5	7.9	14	1.8	0	0.2	0	0.83	0	18	366	78	15
27R-3, 53–58	6	433.9	48.3	16	0.7	10	8.4	13	1.9	0.1	0.2	0	1.41	9	12	366	67	13
28R-1, 54–58	1	440.54	48.7	16	0.6	9.7	8.5	13	1.7	0.1	0.2	0	0.99	0	11	395	71	14
28R-1, 83–87	16	440.83	48.2	17	0.6	9.8	8.1	13	1.7	0.3	0.2	0	1.05	0	0	374	70	14
28R-2, 0–7	1A	441.41	47.7	16	0.6	9.9	9.2	13	1.6	0.1	0.2	0.1	1.65	13	21	340	61	15
29R-1, 0–10	1	449.7	50.1	15	0.9	9.4	8.6	13	2	0.2	0.2	0.1	0.25	16	21	324	93	14
29R-1, 49–53	1	450.19	50.4	15	0.8	9.8	8.8	13	1.9	0.3	0.2	0.1	0.13	13	0	341	93	14
29R-1, 98–100	14	450.68	49.4	17	0.8	8.1	7.8	13	2	0	0.2	0	0.91	26	18	328	80	16
29R-1, 123–126	1	450.93	50.1	16	0.8	9.1	8	13	2	0.2	0.2	0.1	0.35	29	8	384	63	14
29R-2, 1–5	2	451.13	50.1	16	0.8	9.1	8.6	13	2	0.1	0.2	0	0.1	15	0	357	106	14
30R-1, 5–8	1	459.35	50	16	0.8	9.3	8.4	13	2.1	0.1	0.2	0.1	0.03	17	20	366	91	15
30R-1, 81–86	11C	460.11	50.1	15	0.8	9.9	8.8	13	2	0.2	0.2	0.1	0.33	15	0	318	83	14
30R-1, 103–107	1	460.33	50.1	15	0.8	10	8.6	13	2	0.1	0.2	0.1	-0	31	0	368	95	14
30R-1, 137–141	1	460.67	50.4	15	0.8	9.5	8.7	13	2	0.2	0.2	0	0.08	30	25	346	72	13
30R-2, 5–7	1A	460.84	49.7	15	0.8	10	8.4	13	2	0.2	0.2	0.1	0.2	70	0	326	83	15

Notes: Major elements are measured in weight percent (wt%) and trace elements in parts per million (ppm). A value of zero indicates that the element is below the detection limit. LOI = loss on ignition.

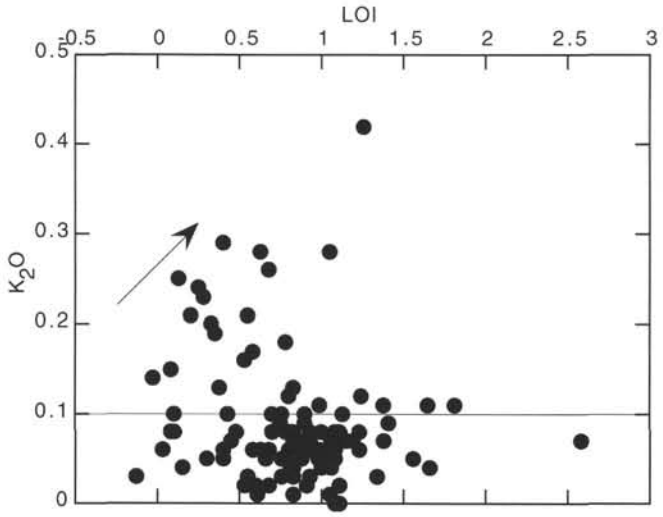

Figure 1. K_2O vs. loss on ignition (LOI) for Hole 896A basalts. Arrow indicates correlation for altered samples (K_2O > 0.1%). Samples with K_2O < 0.1% are classified as unaltered.

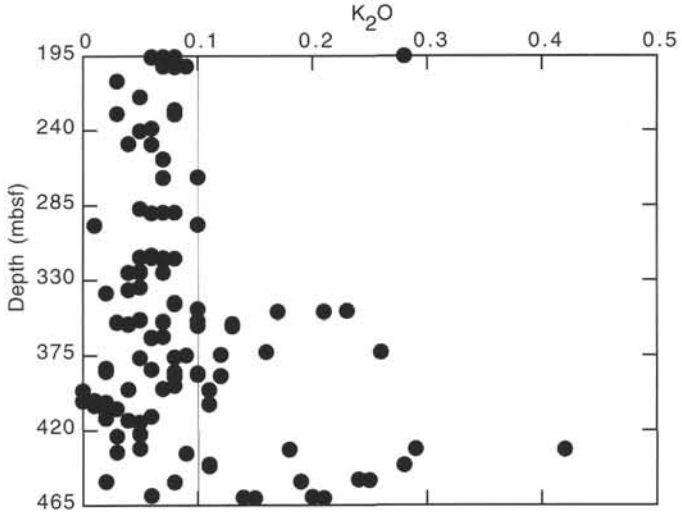

Figure 2. Downhole variation of K_2O in Hole 896A. Basalts with K_2O > 0.10% are classified as altered.

limit (detection limit, 0.1 ppm) and increased the precision of the analysis (± 5%). The increased quality of these data is essential in the petrogenetic discussion as both Rb and Nb are incompatible elements that have been used to both classify Hole 504B basalts (Autio and Rhodes, 1983; Kempton et al., 1985) and to establish the nature of the source of oceanic magmas in general (Sun and McDonough, 1989).

Before discussing the igneous geochemistry of Hole 896A, the effects of alteration must be evaluated because these effects can often mimic magmatic processes (Hellman et al., 1977).

BULK-ROCK ALTERATION

All samples used in the present study were selected so as to exclude obvious signs of alteration (i.e., veined material); however, within Hole 896A all the basalts are passively altered, even though this alteration (<10%) is limited (Alt, Kinoshita, Stokking, et al., 1993). In Hole 896A, bulk-rock alteration of the basalts is limited to three types of halos (Alt, Kinoshita, Stokking, et al., 1993); the halos show no significant variation with depth. However, oxidized alteration correlates with the distribution of massive basalts (Alt, Kinoshita, Stokking, et al., 1993). Because massive units are more abundant below 340 mbsf, oxidative alteration is greater below 340 mbsf (Alt, Kinoshita, Stokking, et al., 1993).

The effects of alteration on the bulk-rock chemistry of pillow basalts have been studied extensively in Hole 504B by Kempton et al. (1985). These authors concluded that K and Sr are mobile in the upper pillow lava section where seawater interaction is greatest. Emmermann (1985) divided the alteration in the pillow lavas into upper oxidative and lower nonoxidative zones, with K_2O, S, and iron oxidation ratio (Fe_2O_3/Fe_2O_3T) being the most effective measures to discriminate between these zones.

In the pillow lavas from Hole 504B, the positive correlation between K_2O and LOI was interpreted as K mobility during the low temperature hydration of the basalts (Dick, Erzinger, Stokking, et al.,

Table 1 (continued).

Core, section, interval (cm)	Piece no.	La	Nb	Ni	Pb	Rb	S	Sc	Sr	Th	U	V	Y	Zn	Zr
26R-1, 134–139	1	0	0.02	201	6	2.35	1210	44	72	2	0	222	22	66	50
26R-2, 88–89	2	0	0.51	185	6	1.7	946	37	86	4	1	208	20	64	48
27R-1, 22–25	1	0	0.72	163	4	2.98	885	39	69	0	0	216	24	65	49
27R-1, 71–75	1	0	0.96	168	3	8.1	327	39	65	0	0	216	21	58	43
27R-1, 86–92	10	0	0.25	146	0	3.79	1510	38	74	5	0	179	20	45	30
27R-1, 101–104	12B	0	0.75	172	0	4.87	846	42	62	5	0	209	23	54	50
27R-2, 109–112	2	4	0.71	170	6	2.26	582	41	69	0	0	200	17	59	32
27R-3, 53–58	6	0	0.42	174	0	2.7	2129	39	62	4	0	192	19	63	35
28R-1, 54–58	1	7	0.52	164	5	2.95	267	38	74	2	0	201	17	57	32
28R-1, 83–87	16	0	0.82	176	0	3.21	522	38	??	5	0	187	18	54	32
28R-2, 0–7	1A	0	0.76	169	0	2.75	653	40	62	1	0	177	18	52	37
29R-1, 0–10	1	0	0.63	134	0	5.36	214	42	54	3	0	250	28	63	43
29R-1, 49–53	1	0	0.75	127	5	6.86	220	46	54	2	0	249	22	66	47
29R-1, 98–100	14	0	0.66	134	0	1.98	1485	39	63	4	0	212	21	45	47
29R-1, 123–126	1	0	0.61	127	5	4.86	135	39	61	0	0	242	23	70	45
29R-2, 1–5	2	4	0.57	186	7	3.16	404	40	60	3	0	229	20	62	47
30R-1, 5–8	1	0	0.89	137	7	2.38	1001	45	63	2	0	236	24	64	45
30R-1, 81–86	11C	0	0.84	132	0	5.7	686	41	55	6	0	232	26	60	47
30R-1, 103–107	1	0	0.92	123	6	5.05	589	42	55	0	0	253	20	65	42
30R-1, 137–141	1	0	1.02	155	7	4.44	273	41	56	0	0	255	23	65	47
30R-2, 5–7	1A	0	0.63	110	0	5.96	682	43	52	3	0	237	26	62	48

Table 2. Comparison of the geochemistry of the basalts from Holes 504B and 896A.

	Hole 504B				Hole 896A	
	Group M	Group D	Group D′	Group T	Upper	Lower
SiO_2	50	50.4	49.9	50.6	49.15	49.35
TiO_2	1.37	0.92	0.92	1.09	0.74	0.85
Al_2O_3	15.3	15.9	15.5	15.3	16.84	16.19
Fe_2O_3	9.95	9.87	10.1	9.86	9.15	9.48
MnO	0.18	0.16	0.19	0.25	0.17	0.18
MgO	8.17	8.4	8.6	8.71	7.64	8.15
CaO	12.5	12.5	13	12.2	13.23	12.74
Na_2O	2.5	2		2.15	1.89	2.02
K_2O	0.06	0.11	0.02	0.03	0.06	0.1
P_2O_2	0.13	0.07	0.07	0.11	0.05	0.05
Rb	<0.5	1.3	<0.5	<0.5	1.9	2.8
Sr	105	64	55	73	67	64
Y	31.2	23.3	22.8	23.5	22	24
Ga	16.2	15.4	15.2	14.8	14.3	14.6
Zr	103.7	47	46	67	43	47
Nb	2.4	0.6	0.9	4.2	0.44	0.65
Zn	79	77	80	107	59	61
Ni	97	117	117	107	159	138
Cr	257	359	336	342	368	344
V	310	274	263	257	230	232

Notes: Data from Hole 504B taken from Kempton et al. (1985). The basalts from Hole 896A have been split into two groups: "Lower" refers to basalts from >340 mbsf, and "Upper" refers to basalts from <340 mbsf.

1992). In Hole 896A, the downhole variation of K_2O is characterized by localized "spikes," which are more common in the lower part of the hole (>340 mbsf), where oxidative groundmass alteration is more extensive (Alt, Kinoshita, Stokking, et al., 1993). Below 340 mbsf, samples with $K_2O > 0.10\%$, display a positive correlation between K_2O and LOI (Fig. 1), where, the LOI values broadly correlate with hydration of the basalts (Alt, Kinoshita, Stokking, et al., 1993). The correlation between LOI and K_2O therefore, indicates the preferential mobility of K during this low temperature alteration. Using this relationship, it is evident that altered samples have $K_2O > 0.10\%$, and that the following pattern to the alteration can be established from the whole rock chemistry:

1. In the upper part (195.1–340 mbsf) alteration effects are limited and the majority of the samples have $K_2O < 0.10\%$ (Fig. 2).
2. Below 340 mbsf, the K_2O curve (Fig. 2) contains several spikes that represent regions of more intense low-temperature alteration. These more altered zones are interspersed with "unaltered" material, suggesting some structural or lithological control to this style of alteration.

Below 340 mbsf in Hole 896A, oxidative alteration of the groundmass, K mobility, massive units, and breccias all increase (Alt, Kinoshita, Stokking, et al., 1993). The relatively high K_2O values are restricted to discrete zones, which appear to correlate with the boundaries of the massive units, suggesting the focusing of fluids and alteration along such lithological boundaries. In contrast, the oxidative alteration of the groundmass is common throughout the majority of the lower part of the hole, within which breccias are more abundant (Alt, Kinoshita, Stokking, et al., 1993). The breccias have the highest porosities within the drilled section (Alt, Kinoshita, Stokking, et al., 1993) which allowed more extensive fluid-rock interactions within this part of the hole, resulting in the oxidation of the groundmass of the basaltic material.

In Hole 504B, Emmermann (1985) suggested that Cu, Zn, S, and Mn were also potential discriminators of alteration. However, in Hole 896A the lack of correlation between these elements and K_2O and LOI suggests that these elements have not been greatly effected by low temperature alteration. Therefore, the most effective chemical discriminate of alteration Hole 896A is K, which suggests that this style of bulk-rock alteration involved interaction with relatively low -temperature seawater (halmyrolysis), which is similar to the style of alteration described from the upper pillow lavas of Hole 504B (Emmermann, 1985). In the subsequent discussion of the igneous geochemistry, the data have been screened for alteration, such that samples with K_2O greater than 0.1% have been excluded.

GEOCHEMICAL OVERVIEW

The basalts in Hole 896A are strongly depleted, moderately evolved mid-ocean ridge basalts (Alt, Kinoshita, Stokking, et al., 1993). The basalts are most similar to the Groups D and D′ basalts described from Hole 504B (Table 2; Autio and Rhodes, 1983; Kempton et al., 1985; Emmermann, 1985). No compositions have as yet been identified that are similar to either the Group M or T basalts described from Hole 504B (Kempton et al., 1985). The drill hole provides a stratigraphy in the lava sequence that may have developed from multiple events of magma injection. Furthermore, each magma pulse may have been produced from a different source, by different degrees of partial melting or from melting columns of different shapes. It is there-

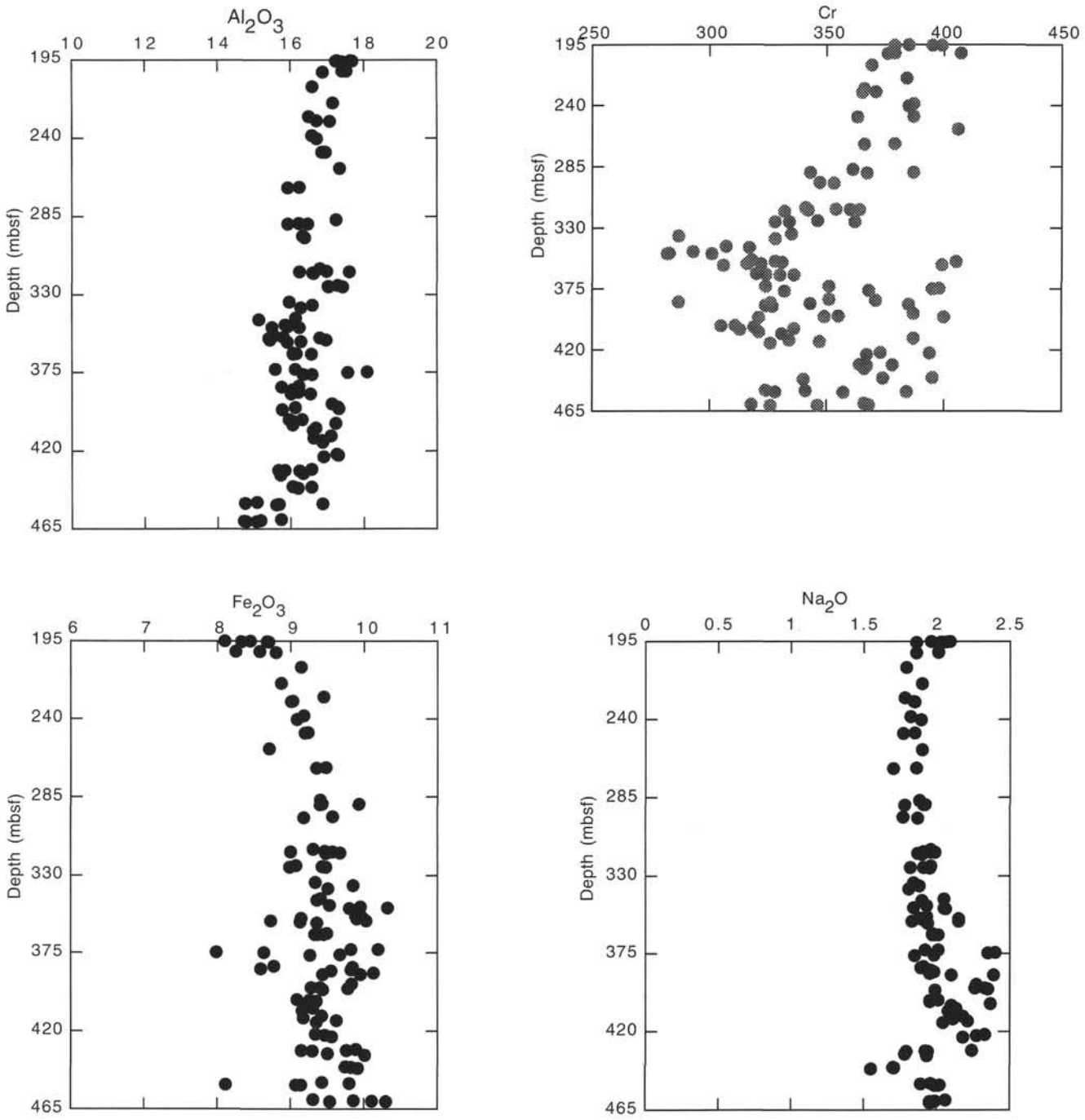

Figure 3. Oxide (wt%) and elemental (ppm) variations downhole in Hole 896A.

fore, critical to establish whether any of the vertical geochemical variation (chemostratigraphy) is attributable to discrete magma batches before discussing the magmatic evolution of the basalt pile as a whole.

CHEMOSTRATIGRAPHY

Basalts from Hole 896A have a relatively restricted compositional range (Alt, Kinoshita, Stokking, et al., 1993), although within the hole there are significant changes in elemental concentrations with depth, which allows the identification of a number of chemical units. The most abrupt change occurs at approximately 340 mbsf (Fig. 3). In the upper part of the hole, in Unit A (195.1–340 mbsf), the basalts have remarkably uniform compositions that are more depleted in TiO_2 than are the Group D and D′ basalts from Hole 504B (Table 2). The lower part of the hole (>340 mbsf) contains the following geochemical units (Fig. 3):

1. Unit B (340–391 mbsf) basalts show no significant variations in TiO_2, V, and Ni, but Cr decreases toward the top of the unit.
2. In Unit C (392–430 mbsf), concentrations of TiO_2, Cr, Ni, and V all decrease systematically toward the top of this unit.

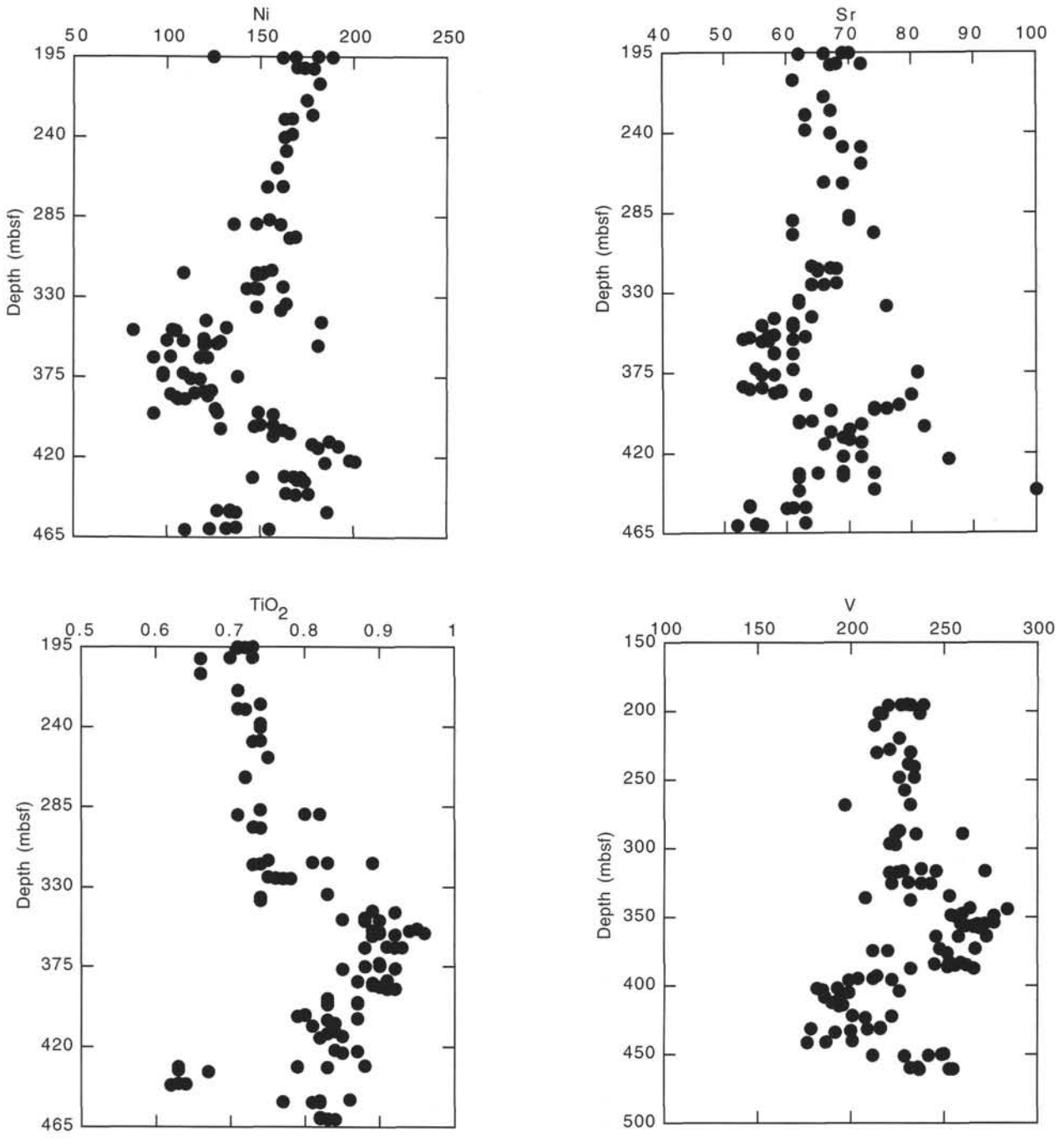

Figure 3 (continued).

3. Unit D (432–434 mbsf) basalts have the lowest TiO_2, Zr, and Y values in the lower part of the hole.
4. Unit E (434 mbsf) basalts have similar compositions to those in Unit B, except that the most primitive compositions occur at the top of this unit.

Incompatible trace element ratios, such as K/Ti, Nb/Zr, and Rb/Zr can be used as indicators of mantle enrichment in ocean floor basalts, because these ratios do not vary greatly with either fractional crystallization and/or extensive partial melting (Sun and McDonough, 1989; Michael et al., 1994). Within Hole 896A the incompatible trace element ratios have a restricted range of values and show no systematic variations with depth, suggesting that the basalts were derived from a similar source. The sawtoothed elemental variations within the drilled section therefore, reflect variations produced by shallower level processes such as magma mixing and fractional crystallization.

In Unit A, the more primitive magmas occur at the top of the unit, suggesting an origin by magma mixing. In contrast, below 340 mbsf, the change in concentrations of Ti, V, Cr, and Ni with depth defines a sawtoothed pattern (Fig. 3). This sawtoothed pattern may result from each unit representing the fractionation of a discrete magma batch, such that following the production of one unit, the magma chamber was replenished and then underwent fractionation. The replenishment introduced a new magma which initially produced rela-

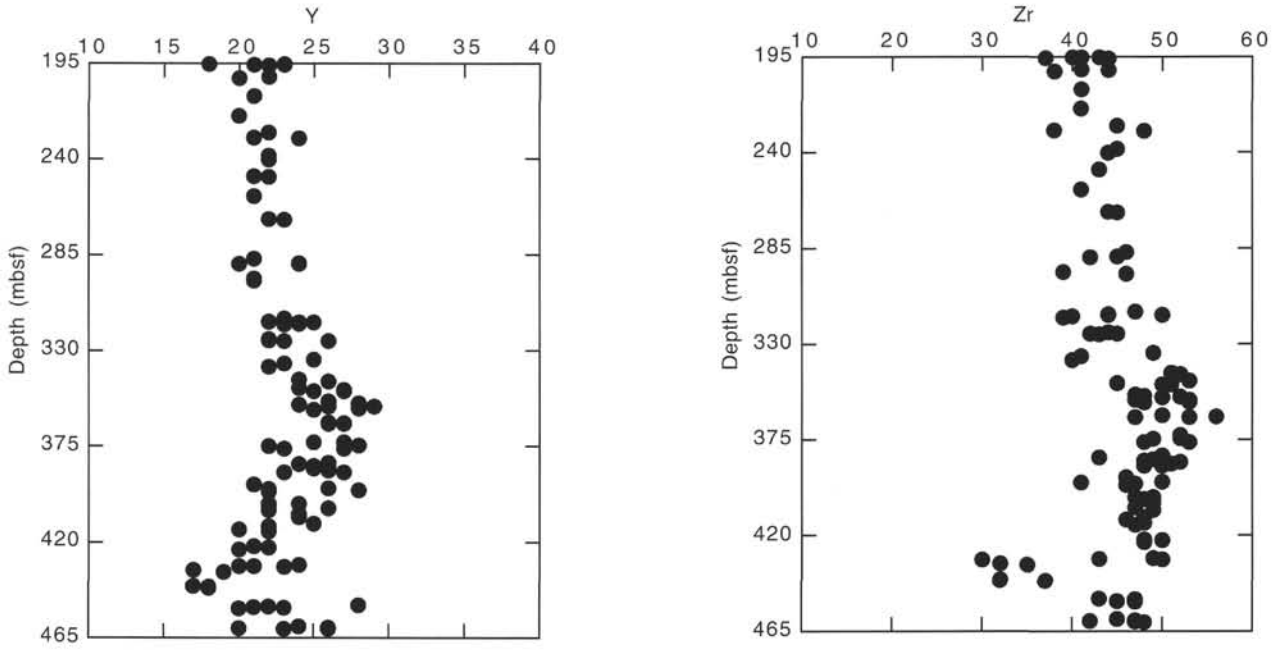

Figure 3 (continued).

tively primitive magmas and then more evolved magmas later. The one exception is Unit E, where the more primitive magmas are at the top of the unit, which indicates an origin by the mixing of magmas.

COMPARISON WITH HOLE 504B

Hole 896A is situated approximately 1 km to the south of Hole 504B, and assuming a spreading rate of 36 mm/yr (Dick, Erzinger, Stokking, et al., 1992) is situated in crust ~2.8 × 104 yr older than the Hole 504B basement. The majority of the volcanism associated with the Costa Rica Rift is situated in a ~2 km wide neovolcanic zone (rift-valley) that is bounded by fault scarps (van Andel and Ballard, 1979). From the difference in age of the two sites, Hole 896A was near to the margin of the neovolcanic zone when the Hole 504B basement was forming. However, the proximity of the two hole does allow assessment of the short term variation in magmatic processes operating at the ridge. As a preliminary guide for such variation the chemostratigraphy of both holes has been constructed (Fig. 4); to facilitate correlation between the holes, all the depth values are expressed as depth into basement for each hole, assuming the basement was first encountered at 179 mbsf in Hole 896A and 274.5 mbsf in Hole 504B (Alt, Kinoshita, Stokking, et al., 1993).

The most significance difference between Holes 896A and 504B occurs in the upper ~150 m. In this region, Hole 896A basalts have higher Al_2O_3 and Ni and lower P_2O_5, TiO_2, V, Y, and Zr values compared with Hole 504B basalts (Fig. 4). The upper ~150 m of basement in Hole 504B is characterized by downhole sawtoothed profiles for Ti and Cr; this region also contains the Group M and T basalts (Kempton et al., 1983). In Hole 896A, the upper ~150 m of basement does not contain any sawtoothed element variations with depth. The sawtoothed profiles are the result of magma mixing, since in a normal fractionating sequence, the most primitive lavas occur at the base and the more evolved at the top, but by mixing of different magma batches it is possible to get the reverse (i.e., most evolved at base, most primitive at top) and so a saw-tooth profile is created within the lava pile. The implication from this data is that during the formation of Hole 504B lavas, the magma chamber was replenished relatively frequently with new (more primitive) magma batches, whereas during the formation of Hole 896A the magma chamber was not replenished on such a relatively short time scale. Below ~150 m in the basement of both holes (Fig. 4), sawtoothed profiles are common, suggesting that the magma chambers were often replenished with new batches of undifferentiated magma.

MAGMATIC EVOLUTION

In Hole 896A, plagioclase and olivine are the major phenocryst phases and clinopyroxene has been reported only as a phenocryst phase between 351 and 391 mbsf (Alt, Kinoshita, Stokking, et al., 1993). Thus, the combination of potential fractionating assemblages can be modeled effectively on major element diagrams (Fig. 5). The following discussions limited to Units A, B and C, since the insufficient unaltered samples in Units D and E to draw any valid conclusions.

Unit A basalts (<340 mbsf) display negative correlations between MgO-CaO and MgO-Al_2O_3, which is consistent with the fractionation of plagioclase and or olivine (Fig. 5). Both Ni and Cr increase toward the top of this unit, indicating a reversed sequence, with the more evolved lavas at the base and the more primitive at top of the unit. Reversed magmatic trends result from magma mixing, which in the case of Hole 896A was the result of mixing a new primitive magma with the evolved fractionated magma remaining in the high level magma chamber.

Overall, basalts from Units B and C display negative correlations between MgO-CaO and MgO-Al_2O_3, and there is a degree of scatter in the data (Fig. 5). This scatter is consistent with the participation of clinopyroxene in the fractionating assemblage (i.e., plagioclase + olivine + clinopyroxene). The involvement of clinopyroxene in the fractionating assemblage is consistent with the phenocryst assemblages described for these basalts (Alt, Kinoshita, Stokking, et al., 1993).

DISCUSSION

The chemostratigraphy for Hole 896A is consistent with the derivation of different magma batches from a common source. However,

significant high-level modification of individual magma batches has occurred by both fractional crystallization and magma mixing. The net result is chemostratigraphy, which reflects the dynamic nature of the magmatic systems. Thus, when viewed as a single entity, the basalts have a range of incompatible trace element concentrations at a given MgO value (Alt, Kinoshita, Stokking, et al., 1993), reflecting the variation of the magmatic processes with time.

There is no evidence to suggest a two-stage fractionation process for the lavas (Grove et al., 1992), but the variation in the nature of the fractionating phases (i.e., presence or absence of clinopyroxene) probably reflects magma chambers located at different levels within the crust or mantle. This model is similar to that proposed by Grove et al. (1992) and suggests that magma chambers on the Costa Rica Rift are dynamic features that shift their location in space and time. Further testing of such a model is being attempted by integrating data from the pillow lavas from Hole 504B, which is situated ~1 km to the north of Hole 896A in crust approximately 2.8×10^4 yr younger than that at Hole 896A.

ACKNOWLEDGMENTS

The analyses used in this study were obtained while TSB was on staff at Nottingham University. NERC also provided funds for TSB to participate on Leg 148 and to attend the post-cruise meeting.

REFERENCES

Alt, J.C., Kinoshita, H., Stokking, L.B., et al., 1993. *Proc. ODP, Init. Repts.*, 148: College Station, TX (Ocean Drilling Program).

Autio, L.K., and Rhodes, J.M., 1983. Costa Rica Rift Zone basalts: geochemical and experimental data from a possible example of multistage melting. *In* Cann, J.R., Langseth, M.G., Honnorez, J., Von Herzen, R.P., White, S.M., et al., *Init. Repts. DSDP*, 69: Washington (U.S. Govt. Printing Office), 729–745.

Dick, H.J.B., Erzinger, J., Stokking, L.B., et al., 1992. *Proc. ODP, Init. Repts.*, 140: College Station, TX (Ocean Drilling Program).

Emmermann, R., 1985. Basement geochemistry, Hole 504B. *In* Anderson, R.N., Honnorez, J., Becker, K., et al., *Init. Repts. DSDP*, 83: Washington (U.S. Govt. Printing Office), 183–199.

Grove, T.L., Kinzler, R.J., and Bryan, W.B., 1992. Fractionation of mid-ocean ridge basalt (MORB). *In* Morgan, J.P., Blackman, D.K., and Sinton, J.M. (Eds.), *Mantle Flow and Melt Generation at Mid-Ocean Ridges*. Geophys. Monogr., Am. Geophys. Union, 71:281–310.

Hellman, P.L., Smith, R.E., and Henderson, P., 1977. Rare earth element investigation of the Cliefden Outcrop, N.S.W., Australia. *Contrib. Mineral. Petrol.*, 65:155–164.

Hey, R., Johnson, G.L., and Lowrie, A., 1977. Recent plate motions in the Galapagos area. *Geol. Soc. Am. Bull.*, 88:1385–1403.

Holden, J.C., and Dietz, R.S., 1972. Galapagos Gore, NazCoPac Triple Junction and Carnegie/Cocos Ridges. *Nature*, 235:266–269.

Kempton, P.D., Autio, L.K., Rhodes, J.M., Holdaway, M.J., Dungan, M.A., and Johnson, P., 1985. Petrology of basalts from Hole 504B, Deep Sea Drilling Project, Leg 83. *In* Anderson, R.N., Honnorez, J., Becker, K., et al., *Init. Repts. DSDP*, 83: Washington (U.S. Govt. Printing Office), 129–164.

Lonsdale, P., and Klitgord, K.D., 1978. Structure and tectonic history of the eastern Panama Basin. *Geol. Soc. Am. Bull.*, 89:981–999.

Michael, P.J., Forsyth, D.W., Blackman, D.K., Fox, P.J., Hanan, B.B., Harding, A.J., MacDonald, K.C., Neuman, G.A., Orcutt, J.A., Tolstoy, M., and Weiland, C.M., 1994. Mantle control of a dynamically evolving spreading centre: Mid-Atlantic Ridge 31–34°S. *Earth Planet. Sci. Lett.*, 121:451–468.

Sun, S.-S., and McDonough, W.F., 1989. Chemical and isotopic systematics of oceanic basalts: implications for mantle composition and processes. *In* Saunders, A.D., and Norry, M.J. (Eds.), *Magmatism in the Ocean Basins*. Geol. Soc. Spec. Publ. London, 42:313–345.

Tual, E., Jahn, B.M., Bougault, H., and Joron, J.L., 1985. Geochemistry of basalts from Hole 504B, Leg 83, Costa Rica Rift. *In* Anderson, R.N., Honnorez, J., Becker, K., et al., *Init. Repts. DSDP*, 83: Washington (U.S. Govt. Printing Office), 201–214.

Van Andel, T.H., and Ballard, R.D., 1979. The Galapagos Rift at 86°W: 2. Volcanism, structure and evolution of the rift valley. *J. Geophys. Res.*, 84:5379–5406.

Date of initial receipt: 8 August 1994
Date of acceptance: 21 July 1995
Ms 148SR-101

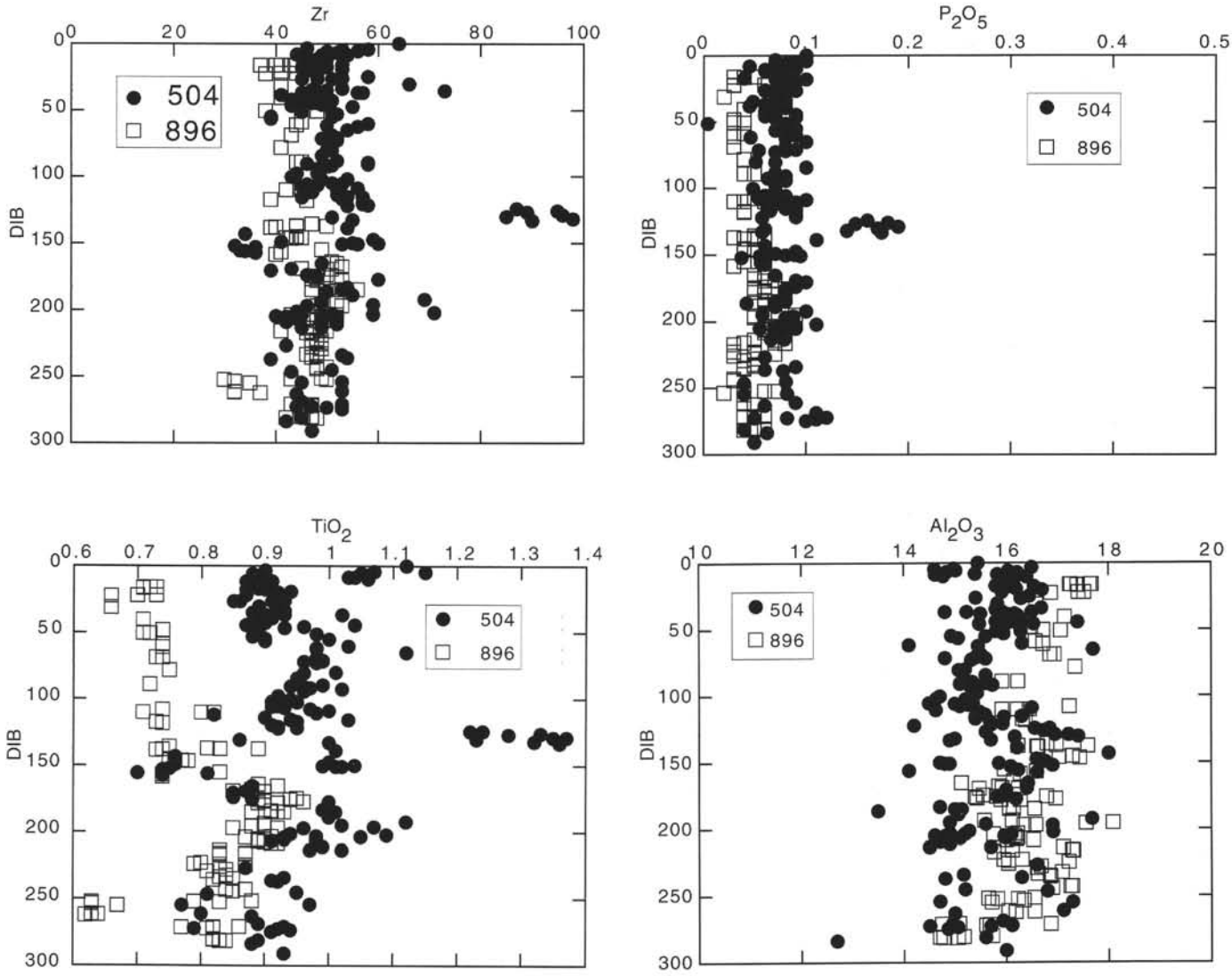

Figure 4. Oxide (wt%) and elemental variations within Holes 896A and 504B. The depth scale is expressed as depth into basement (DIB) to allow direct comparison between the two holes. Data for Hole 504B from Emmermann (1985), Kempton et al. (1985), and Tual et al. (1985).

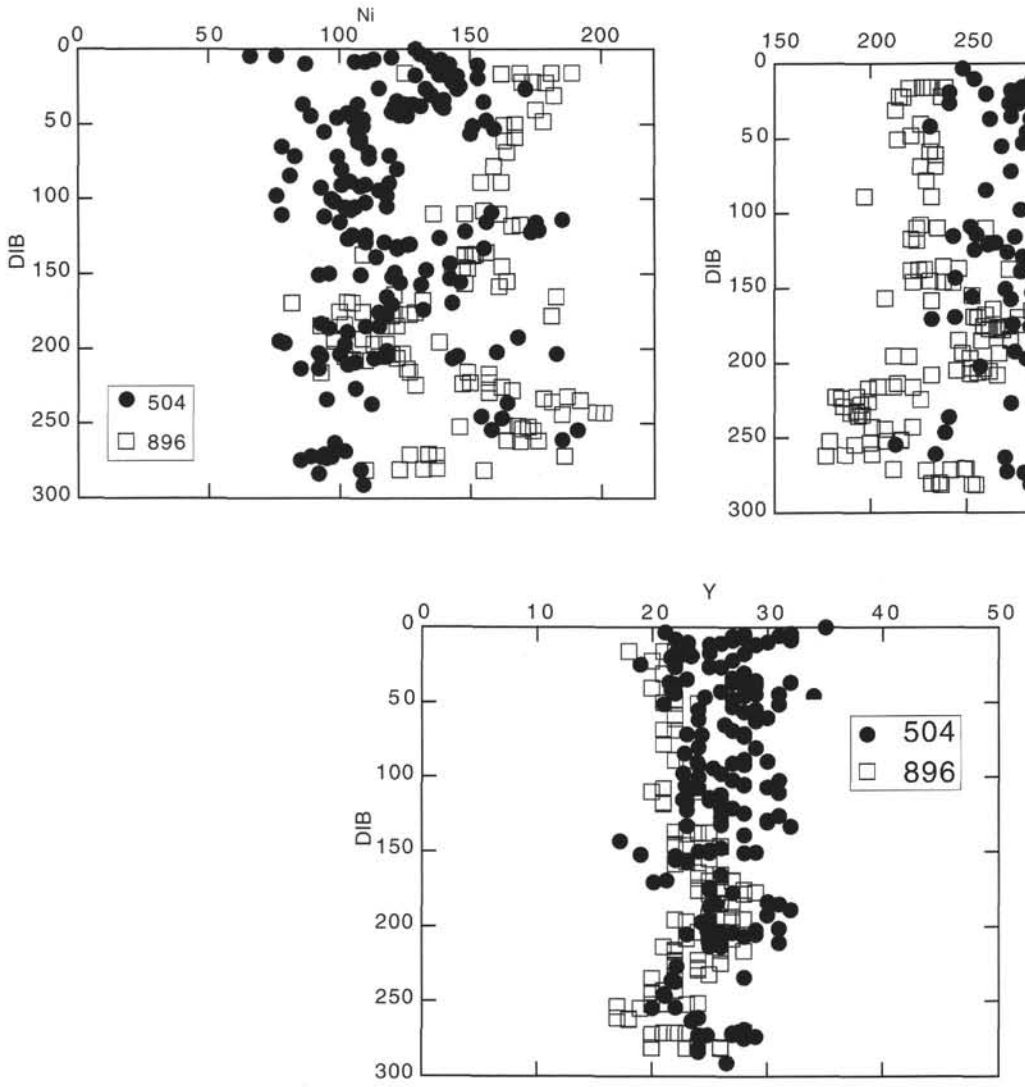

Figure 4 (continued).

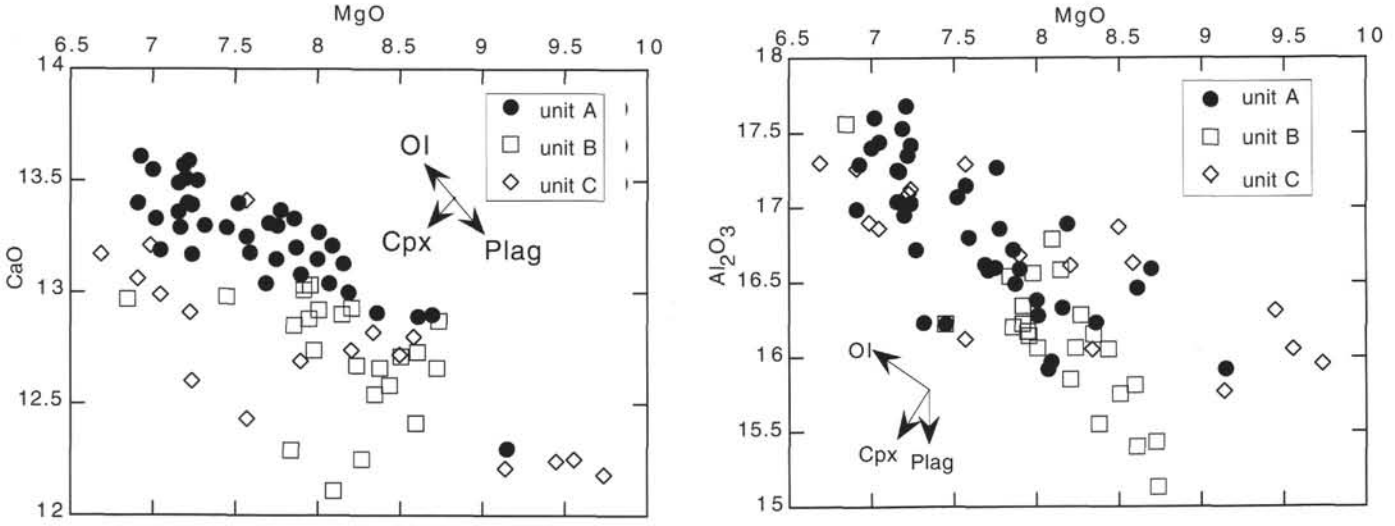

Figure 5. MgO vs. CaO and Al_2O_3 for basalts from Hole 896A. Fractionation vectors calculated for olivine (Ol), plagioclase (Plag), and clinopyroxene (Cpx).